Environmental Science & Technology

Article

pubs.acs.org/est

Volatility of Organic Molecular Markers Used for Source Apportionment Analysis: Measurements and Implications for Atmospheric Lifetime

Andrew A. May, Rawad Saleh, Christopher J. Hennigan, Neil M. Donahue, and Allen L. Robinson*

Center for Atmospheric Particle Studies, Carnegie Mellon University, 5000 Forbes Avenue, Pittsburgh, Pennsylvania 15213, United States

Supporting Information

ABSTRACT: Molecular markers are organic species used to define fingerprints for source apportionment of ambient fine particulate matter. Traditionally, these markers have been assumed to be stable in the atmosphere. This work investigates the gas-particle partitioning of eight organic species used as molecular markers in receptor models for biomass burning (levoglucosan), motor vehicles (5α-cholestane, *n*-hexacosane, *n*-triacontane, 1,2-benz[*a*]-anthracene, coronene), and meat cooking (cholesterol, oleic acid). Experiments were conducted using a thermodenuder to measure the evaporation of single component particles. The data were analyzed using the integrated volume method to determine saturation concentrations and enthalpies of vaporization for each compound. The results indicate that appreciable quantities (>10%) of most of these markers exist in the gas phase under typical atmospheric conditions. Therefore, these species should be considered semivolatile. Predictions from a chemical kinetics model indicate that gas-particle partitioning has important effects on the atmospheric lifetime of these species. The atmospheric decay of semivolatile compounds proceeds much more rapidly than nonvolatile compounds because gas-phase oxidation induces evaporation of particle-phase material. Therefore, both gas-particle partitioning and chemical reactions need to be accounted for when semivolatile molecular markers are used for source apportionment studies.

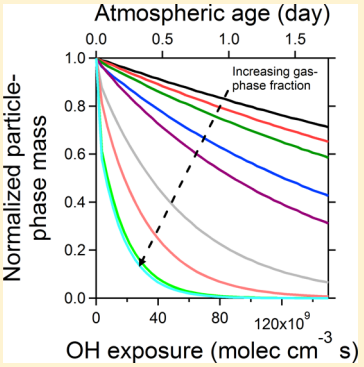

INTRODUCTION

Individual organic compounds (molecular markers) are often used to apportion ambient particulate matter (PM) to sources. Examples of molecular markers include hopanes and steranes, polycyclic aromatic hydrocarbons, and levoglucosan. Source apportionment analyses typically assume that these compounds are stable in the atmosphere; that is, they are nonvolatile and nonreactive.[1] However, recent work has shown that many organic molecular markers can be oxidized over atmospherically relevant time scales;[2] there is also evidence that some markers may be semivolatile at atmospheric conditions. For example, Sihabut et al.[3] report significant concentrations of molecular markers (*n*-alkanes and hopanes) on backup filters, implying that these species are semivolatile. Furthermore, mild heating (+ 10 K) can cause significant evaporation of many molecular markers (*n*-alkanes, hopanes, steranes, cholesterol, levoglucosan) from quartz filter samples of ambient aerosols.[4] This suggests that several commonly used molecular markers are semivolatile; however, little work has directly quantified the volatility of these species and its effect on atmospheric lifetime.

The gas-particle partitioning of molecular markers depends on thermodynamic properties including subcooled liquid saturation concentration (C_i^o) and enthalpy of vaporization ($\Delta H_{vap,i}$). Thermodynamic data exist for some classes of organic species found in organic aerosol (e.g., mono- and dicarboxylic acids, alkanols, sterols, sugars).[5−14] Some of these species are used as molecular markers. These data suggest that many molecular markers may be semivolatile, but uncertainties remain. Challenges include (1) extrapolating thermodynamic properties measured at high experimental temperatures (~350−450 K) to ambient temperature, and (2) accounting for potential mass transfer resistance (i.e., the mass accommodation coefficient α) when deriving property data from experiments based on evaporation rates. For example, mass transfer resistance can lead to the under-estimation of the volatility of the aerosol.

The atmospheric lifetime of molecular markers (and thus their suitability for use in receptor models) likely depends on their gas-particle partitioning. For oxidation by OH radicals, gas-phase reactions are often much faster than heterogeneous reactions because heterogeneous OH uptake is diffusion limited.[15] Therefore, oxidation of organic vapors will drive evaporation of particle-phase semivolatile compounds, potentially causing rapid depletion of molecular marker concentrations. For example, laboratory studies report that the oxidation rates of 5α-cholestane and levoglucosan exceed the theoretical maximum reaction rate for heterogeneous chemistry.[16−19] The authors of those studies hypothesized that the

Received: June 6, 2012
Revised: September 18, 2012
Accepted: September 26, 2012
Published: September 26, 2012

Table 1. List of Molecular Markers Studied and Measured Thermodynamic Properties

			current work			prior work[b]		
species	chemical formula	source	C_i^o (298 K) (μg m^{-3})	P_i^{vap} (Pa)	$\Delta H_{vap,i}$ (kJ mol^{-1})	C_i^o (298 K)[a] (μg m^{-3})	P_i^{vap} (Pa)	$\Delta H_{vap,i}$ (kJ mol^{-1})
levoglucosan	$C_6H_{10}O_5$	biomass burning[57]	13 ± 2	2.0×10^{-4}	101 ± 3	6.0 (345−405 K);[13] 12 (298−318 K)[5]	9.2×10^{-5};[13] 1.8×10^{-4} [5]	100;[13] 52[5]
cholesterol	$C_{27}H_{46}O$	meat cooking[58]	0.037 ± 0.022	2.4×10^{-7}	136 ± 8	0.011* (544−574 K);[11] 0.0035* (387−413 K)[12]	7.1×10^{-8}*[11]; 2.3×10^{-8}* [12]	148*[11]
oleic acid	$C_{18}H_{34}O_2$	meat cooking[58]	6.6 ± 0.8	5.8×10^{-5}	103 ± 5	2.5 (298 K);[35] 0.85 (293−328 K);[14] 0.25 (305−340 K);[6] 5.0 (301−321 K)[34]	2.2×10^{-5};[35] 7.5×10^{-6};[14] 2.2×10^{-6};[6] 4.4×10^{-5} [34]	143;[6] 105[34]
5α-cholestane	$C_{27}H_{48}$	unburned motor oil[1]	0.38 ± 0.01	2.5×10^{-6}	153 ± 4	0.29 (392−462 K)[10]	1.9×10^{-6}* [10]	135[10]
n-hexacosane	$C_{26}H_{54}$	vehicle exhaust[59]	0.27 ± 0.05	1.8×10^{-6}	146 ± 8	0.42 (509−560K)[27]	2.8×10^{-6} [27]	132[27]
n-triacontane	$C_{30}H_{62}$	vehicle exhaust[59]	0.0072 ± 0.0033	4.2×10^{-8}	152 ± 6	0.0057 (529−568 K)[27]	3.4×10^{-8} [27]	152[27]
1,2-benz[*a*] anthracene	$C_{18}H_{12}$	natural gas combustion[1]	9.2 ± 0.8	1.0×10^{-4}	106 ± 0.8	3.8 (323−473 K);[9] 14 (545−575 K)[8]	4.1×10^{-5};[9] 1.5×10^{-4} [8]	106[8]
coronene	$C_{24}H_{12}$	gasoline vehicle exhaust[59]	3.9 ± 1.7	3.2×10^{-5}	142 ± 13	0.081 (323−473 K);[9] 20.1* (430−555 K);[37] 0.00011* (421−504 K)[36]	6.7×10^{-7};[9] 1.7×10^{-4}*;[37] 9.1×10^{-10}* [36]	104;[9] 123[7]

[a]Temperature range over which previous studies measured properties. [b]All values assumed to be subcooled liquid properties except where marked by an (*), indicating the solid value (derived from a Knudsen effusion technique from a crystalline compound).

dx.doi.org/10.1021/es302276t | Environ. Sci. Technol. 2012, 46, 12435−12444

unexpectedly rapid oxidation was due to the molecular markers being semivolatile; hence, gas-phase oxidation will occur.

This paper quantifies important thermodynamic properties affecting gas-particle partitioning (saturation concentration and enthalpy of vaporization) for eight organic compounds that have been used as molecular markers for source apportionment studies. We apply the integrated volume method (IVM)[20] to derive the saturation concentration (C_i^o at 298 K) and enthalpy of vaporization ($\Delta H_{vap,i}$) of the compounds from measurements of evaporation from single component particles in a thermodenuder operating between 20 and 80 °C (thus including ambient temperature). We then explore the atmospheric implications of using semivolatile compounds as molecular markers using a model that accounts for coupled chemical reaction/gas-particle partitioning kinetics.

MATERIALS AND METHODS

Evaporation experiments using a thermodenuder were conducted in triplicate to collect data to infer the saturation concentration and enthalpy of vaporization of the organic compounds listed in Table 1. The list includes molecular markers for biomass burning, motor vehicle, and meat cooking emissions. Seven of these compounds were identified in ambient PM by a recent study;[4] although it was not quantified in this ambient study, oleic acid was also selected since it is used as a tracer for cooking emissions.[2] Compounds were purchased from Fisher Scientific (Waltham, MA); all had specified purity of 97% or greater. No additional purification was performed; it was assumed that slight impurities would not have a significant effect on the measurement of the thermodynamic properties.

A schematic of the experimental setup is shown in Figure 1. Single-component aerosols were generated by atomizing

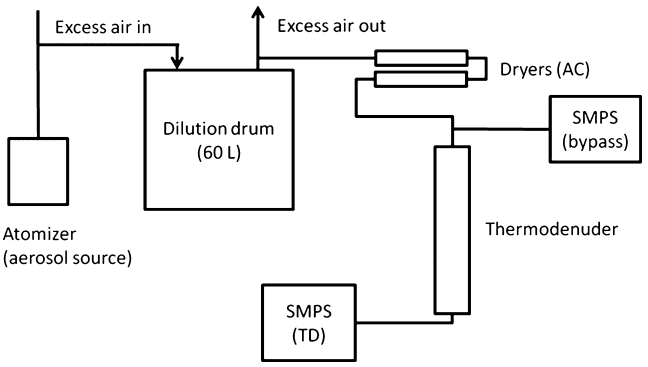

Figure 1. Setup for integrated volume experiments. Single-component aerosol is generated by the atomizer; this aerosol mixes with conditioned excess air in a dilution drum and later passes through diffusion dryers to promote solvent evaporation. Dryers contained activated carbon (AC) to remove organic solvents. Scanning mobility particle sizers (SMPS) were used to quantify aerosol volume concentrations upstream and downstream of the thermodenuder (TD).

solutions containing 0.2 wt % of the molecular marker species dissolved in organic solvents using a commercial atomizer (TSI 3076; TSI, Inc., Shoreview, MN); we assume that we generated subcooled liquid aerosol. Following the method of Veranth et al.,[21] the alkanes and polycyclic aromatic hydrocarbons (PAHs) were dissolved in *n*-hexane (20% v/v) or toluene (30% v/v), respectively; the balance of the solution was reagent alcohol (90% ethanol, 5% methanol, 5% iso-propanol by volume; histological-grade; Fisher Scientific). Levoglucosan, cholesterol, and oleic acid were dissolved in 100% reagent alcohol.

Downstream of the atomizer, the aerosol and an excess dilution flow of conditioned (HEPA- and activated-charcoal-filtered) air at 35 Lpm were passed into a 60-L mixing drum to promote solvent evaporation. The conditioned air was not treated to remove water vapor as the supply line typically has RH < 5%. A 2-Lpm sample was drawn from the drum through activated-charcoal diffusion dryers to remove any residual solvent. Increasing the excess flow of dilution air above 35 Lpm did not change the mode of the particle size distribution; therefore, the system appeared to achieve near-complete solvent evaporation, though minute amounts of residual solvent may have remained. Any residual solvent should not affect the inferred thermodynamic properties.[22]

After drying, the aerosol was sent to either a reference scanning mobility particle sizer (SMPS; TSI 3081/3010) to characterize the aerosol size distribution at ambient temperature or through a thermodenuder and a second SMPS (TSI 3081/3772). A thermodenuder (TD) is a stainless steel tube that is heated to a range of temperature set points, inducing aerosol evaporation, followed by an activated carbon denuder to remove the evaporated vapors. The TD used in this study had a t_{res} of 16.7 s at room temperature. Switching the reference SMPS with the sampling SMPS had negligible effects on the derived thermodynamic properties (e.g., for levoglucosan, C_i^o (298 K) = 11.9 μg m^{-3} vs 14.7 μg m^{-3} which is within the measurement uncertainties of ± ~10% in the SMPS).

The data were analyzed using the integrated volume method (IVM).[20] If the aerosol reaches equilibrium within the thermodenuder, the change in aerosol mass inside the TD can be expressed as:

$$\Delta M_i(T_{TD}) = C_i^o(298\ \mathrm{K})\cdot\left\{\exp\left[-\frac{\Delta H_{vap,i}}{R}\left(\frac{1}{T_{TD}}-\frac{1}{298\ \mathrm{K}}\right)\right]-1\right\} \quad (1)$$

where $\Delta M_i(T_{TD})$ is the difference in aerosol mass concentration between the inlet and outlet stream of the TD, C_i^o (298 K) is the subcooled liquid saturation concentration of the species at 298 K, $\Delta H_{vap,i}$ is the enthalpy of vaporization of the species, and R is the ideal gas constant. ΔM_i values were calculated from the SMPS volume concentrations (ΔV_i) assuming spherical particles and densities of 0.8 g cm^{-3} for *n*-alkanes, 1.2 g cm^{-3} for PAHs, 1.5 g cm^{-3} for levoglucosan (assuming it has a similar density to glucose), and 0.9 g cm^{-3} for 5α-cholestane, cholesterol, and oleic acid.[23] While the calculated C_i^o (298 K) depends on the assumed density, actual densities are unlikely to vary significantly from these assumed values. Consequently, uncertainty in density should not affect our determination of whether a molecular marker is semivolatile. For example, if the density of levoglucosan is 1.8 g cm^{-3} (not 1.5 g cm^{-3}), the estimated saturation concentration of levoglucosan would increase by only a factor of 1.2.

Thermodynamic properties were determined using data collected by operating the TD over a range of temperatures to obtain a range of measured ΔM_i values. A least-squares fit on the data collected from each experiment was then performed using eq 1 to determine the thermodynamic properties of the compound (C_i^o (298 K) and $\Delta H_{vap,i}$) that best describe the set of measured ΔM_i.

The IVM requires that the aerosol reach equilibrium. Therefore, a key advantage of the approach is that it requires

no assumptions on the properties that control aerosol evaporation rate such as the mass accommodation coefficient. To ensure that the aerosol reaches equilibrium in the TD, the residence time in the system should be greater than the equilibration time of the aerosol τ, which is governed by the aerosol condensation sink (CS):

$$\tau = CS^{-1} = (2\pi N_t d_p DF)^{-1} \quad (2a)$$

$$F = \frac{1 + Kn}{1 + 0.3773Kn + 1.33Kn\frac{1+Kn}{\alpha}} \quad (2b)$$

where N_t is the total aerosol number concentration, d_p is the mass-median particle size (assumed monodisperse), D is the diffusion coefficient for the organic vapors in air (assumed to be 5×10^6 m^2 s^{-1}),[24] Kn is the Knudsen number (= $2\lambda/d_p$, where λ = 65.2 nm, the mean free path of organic molecules in air at 1 atm and 25 °C), and α is the mass accommodation coefficient. Saleh et al.[25] propose a semiempirical guideline that equilibrium is approached if the residence time in the thermodenuder is at least five times greater than τ (~95% of equilibrium). This condition has been nearly met for all experiments using α = 1 (Figure S1). If the mass accommodation coefficient were less than unity (which introduces mass transfer limitations to the system), equilibrium will not be attained; even so, our results would provide a lower bound of C_i^o (298 K) for the tested compounds, since the measurements would have underestimated the equilibrium ΔM_i. Experiments where $t_{res}:\tau$ < ~5 provide consistent thermodynamic properties to experiments with $t_{res}:\tau$ > ~5 (5α-cholestane) or to previously published literature (n-triacontane; 1,2-benz[a]anthracene); we discuss this further in the Supporting Information. The equilibrium condition was also assessed through predictions from an equilibrium model (eq 4 below) and an evaporation kinetics model[24] with α = 1, which both agree very well with experimental data (Figure S2).

EXPERIMENTAL RESULTS

Thermodynamic Properties. Thermodenuder data for three compounds are presented in Figure 2, which presents the measured evaporated aerosol mass concentration (ΔM_i) as a function of thermodenuder temperature (similar plots for the other compounds are contained in the Supporting Information). There is some scatter in the data in Figure 2; it is due to small fluctuations in the organic aerosol concentration (C_{OA}) exiting the dilution drum along with measurement uncertainties in the SMPS (±3% in particle sizing; ± 10% in particle number concentration). There may also be a slight temperature dependence to the variability in the data as residual solvent should evaporate before any of the organic compounds listed in Table 1. This variability could also explain the presence of negative values in the data, which occur prior to aerosol evaporation in the TD. Finally, the data were corrected for particle number losses in the thermodenuder due to diffusion and thermophoresis (see Supporting Information for details).

Thermodynamic properties were determined for each experiment by fitting eq 1 to the data using a least-squares approach. Values of C_i^o (298 K) and $\Delta H_{vap,i}$ were derived for each of the three experiments for each molecular marker; average values (n = 3) from these three fits along with standard deviation are reported in Table 1. Model predictions using the mean C_i^o (298 K) and $\Delta H_{vap,i}$ values are shown in Figure 2.

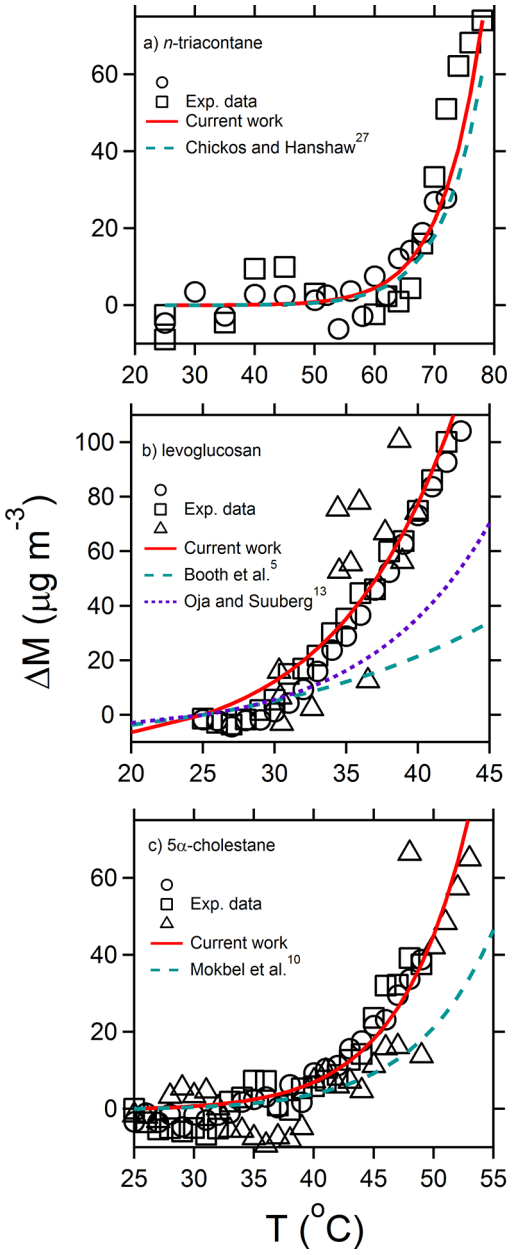

Figure 2. Thermodenuder data for (a) n-triacontane, (b) levoglucosan, and (c) 5α-cholestane. Curves indicate model predictions using eq 1 and the thermodynamic properties listed in Table 1. Different symbols represent independent experiments. Negative values of ΔM are likely attributed to measurement uncertainty in the SMPS.

Figure 2a presents results for n-triacontane (C_{30} n-alkane) to demonstrate the performance of the system. Many previous studies have estimated n-alkane saturation vapor pressures.[26−31] Figure 2a demonstrates that there is good agreement between our n-triacontane properties and the previously published thermodynamic data, indicating that our results are not significantly affected by the scatter in the data; this agreement with n-alkane data is also demonstrated for n-hexacosane in Figure S2.2.

Results for levoglucosan (a biomass burning marker) and 5α-cholestane (a motor vehicle marker) are shown in Figure 2b and 2c, respectively. Both pure levoglucosan and pure 5α-cholestane particles evaporate significantly with heating from 25

to 45 °C. However, Figure 2 indicates that 5α-cholestane has a lower ΔM_i than levoglucosan, suggesting that it is less volatile.

Donahue et al.[32] define semivolatile organic compounds to have 0.3 < C_i^* < 300 μg m^{-3}. We can relate C_i^o to C_i^* through the following relationship, accounting for nonideal solutions:[32]

$$C_i^* = \zeta_i C_i^o \quad (3)$$

where ζ_i is a mass-based activity coefficient of species i in the organic aerosol (OA) solution. The results in Table 1 suggest than several commonly used molecular markers are semivolatile as pure components and in ideal solutions (ζ_i = 1). If the solution is nonideal ($\zeta_i \neq 1$), then components will appear more or less volatile than the ideal case. When ζ_i > 1, gas-particle partitioning is shifted toward the gas phase. This can occur, for example, when a nonpolar compound partitions into a more polar aerosol matrix.[32]

In a complex aerosol mixture, the mass fraction of any individual organic species will typically be far less than unity. This dilution effect is described using the following model for equilibrium absorptive gas-particle partitioning of semivolatile organics:[33]

$$\xi_i = \left(1 + \frac{C_i^*(T)}{C_{OA}}\right)^{-1} \quad (4)$$

where ξ_i is the fraction of material in the particle phase and C_{OA} is the OA concentration. C_i^* is a function of temperature following the Clausius−Clapeyron equation. We can predict the fraction of an organic species that exists in the vapor phase (1-ξ_i) using eq 4. For example, at 298 K with C_{OA} = 10 μg m^{-3} and assuming ζ_i = 1, almost 60% of levoglucosan (C_i^o (298 K) = 13 μg m^{-3}) and 4% of 5α-cholestane (C_i^o (298 K) = 0.38 μg m^{-3}) will exist as vapors. For a more dilute system (C_{OA} = 1 μg m^{-3}), ∼90% of levoglucosan and ∼30% of 5α-cholestane will exist in the gas phase.

Comparison with Literature Data. Table 1 summarizes the measured thermodynamic properties and compares them to previous work. Literature data for saturation vapor pressures measured using correlation gas chromatography (subcooled liquid vapor pressure) by Chickos and Hanshaw[26] (*n*-triacontane in Figure 2a and *n*-hexacosane in Figure S2d) and Hanshaw et al.[8] (1,2-benz[*a*]anthracene in Figure S2e) generally agree very well with results from the IVM approach. The data for oleic acid agree very well with measurements by Safieddine[34] who also performed IVM experiments (Figure S2a) and reasonably well with data from other studies.[6,14,35]

Our data for coronene (C_i^o (298 K) = 3.9 μg m^{-3}) fall within the wide range of values reported in the literature. Prior studies report values from 1.1 × 10^{-4} μg m^{-3} [36] to 20.1 μg m^{-3} [37] for C_i^o (298 K) over a solid inferred from experiments using a Knudsen effusion technique. However, C_i^o values less than ∼0.1 μg m^{-3} require a $\Delta H_{vap,i}$ of nearly 250 kJ mol^{-1}—a value much greater than reported enthalpies of sublimation[36]—to reproduce our experimental data for coronene (Figure S3c). Therefore, the lower end of the literature results is not consistent with our results. The exact cause of this discrepancy is unknown.

Less is known about volatility of molecular markers such as levoglucosan and 5α-cholestane. Figure 2b compares levoglucosan data to predictions based on the thermodynamic properties reported by Oja and Suuberg[13] and Booth et al.[5] Figure 2c compares the 5α-cholestane data to predictions based on the properties of Mokbel et al.[10] For both compounds, previous results predict less evaporation than our measurements. Likely explanations include that both Oja and Suuberg[13] and Mokbel et al.[10] heated samples past the melting point, and therefore, inferred thermodynamic properties at high temperatures (∼345−460 K). The discrepancy with our results may simply reflect the uncertainty in extrapolation from high experimental temperatures to ambient temperature. Nevertheless, the prior data also support the conclusion that these molecular markers are semivolatile.

Data from biomass burning experiments also support the conclusion that levoglucosan evaporates from ambient particles, and hence, is semivolatile. Figure 3 presents thermodenuder measurements performed on biomass burning primary organic aerosol (POA).[38−40] The plot shows the mass fraction remaining (MFR) of the m/z 60 mass fragment measured using a quadrupole aerosol mass spectrometer (AMS):

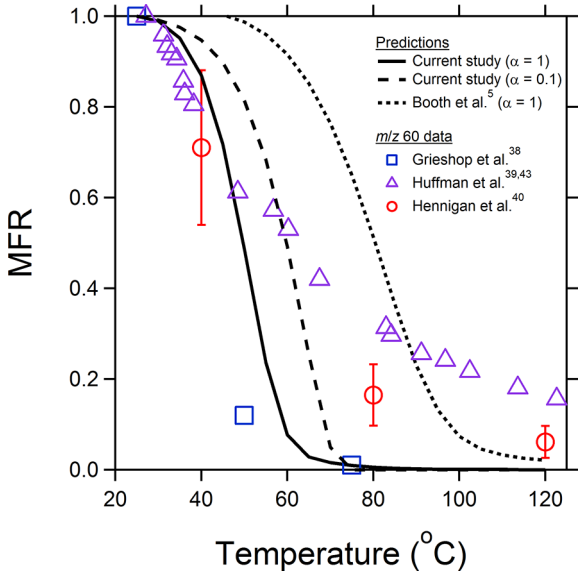

Figure 3. Measured and predicted evaporation of levoglucosan in biomass smoke particles as a function of thermodenuder temperature. MFR = Mass fraction remaining (see text). Measured data are based on aerosol mass spectrometer signal at m/z 60 from Grieshop et al.[38] Huffman et al.[39] and Hennigan et al.[40] Model predictions are made using the properties for levoglucosan (Table 1) and Booth et al.,[5] using an evaporation kinetics model with α specified in the legend. Other assumptions are discussed in the text.

$$MFR = \frac{C_{m/z60}(T_{TD})}{C_{m/z60}(T_{amb})} \quad (5)$$

where $C_{m/z\ 60}(T_{TD})$ and $C_{m/z\ 60}(T_{amb})$ are the m/z 60 signal at the thermodenuder temperature and ambient temperature (∼25 °C), respectively. m/z 60 is produced from the fragmentation of anhydrosugars such as levoglucosan, mannosan, and galactosan, which are emitted during biomass combustion.[41] Figure 3 shows that the AMS m/z 60 signal rapidly decreases with heating, reaching a T_{50} (temperature at which the m/z 60 signal has fallen by 50%) between 40 and 65 °C, depending on the data set.

Figure 3 also shows predictions of the evaporation of levoglucosan for the conditions inside the thermodenuder using the new thermodynamic properties listed in Table 1. The calculations were performed with the evaporation kinetics model of Riipinen et al.[24] The model uses input values of C_{OA} =

30 μg m^{-3} and d_p = 350 nm, the average experimental conditions from the prior studies, with a TD residence time of 18.6 s. The volatility distribution and enthalpies of vaporization of bulk biomass burning POA emissions are from Grieshop et al.[42] If α = 1 (solid line in Figure 3), the model reproduces the full range of m/z 60 MFR data from Hennigan et al.[40] and Grieshop et al.[38] as well as roughly the first half of the data from Huffman et al.,[39,43] only missing the tail at high temperature. This tail could indicate compounds other than levoglucosan contributing to the AMS m/z 60 fragment ion signal;[44] however, it may also be caused by differences in the *CS* and residence time in the thermodenuder during experimentation. The model can also reproduce the data in Figure 3 reasonably well using α = 0.1 (dashed line), although there is a slight increase in the discrepancy between measurements and predictions compared to α = 1. In contrast, the model cannot reproduce the data using the thermodynamic properties derived by Booth et al.[5] (dotted line in Figure 3), as the prediction indicates that levoglucosan should be less volatile than is observed.

Our results are also qualitatively consistent with ambient filter measurements. Sihabut et al.[3] measured *n*-alkane and hopane concentrations on backup quartz filters. For example, ~25% of the total *n*-hexacosane mass and ~6% of the total *n*-triacontane mass were detected on the backup filter; furthermore, ~11% of the total mass of trisnorhopane (C_{27} hopane, which likely has a C_i^o (298 K) similar to 5α-cholestane, a C_{27} sterane) was detected on the backup filter. Since these compounds are identified on the backup filters, they are likely collected as adsorbed vapors, implying that they are semivolatile. Ruehl et al.[4] report that a 10 K temperature increase resulted in the evaporation of a significant amount of certain *n*-alkanes, hopanes, and steranes from a quartz filter. In fact, the Ruehl et al.[4] measurements suggest that *n*-alkanes and steranes in ambient aerosol partition to the gas phase even more than predicted by the pure component data in Table 1 (i.e., $\zeta_i > 1$ for these compounds partitioning into atmospheric aerosols). Unfortunately, quantitative comparisons between our data and the filter measurements cannot be made because of uncertainties associated with sampling artifacts as well as the mixing state of ambient OA.

Atmospheric Implications. *Particle-Phase Decay.* Given that the data in Table 1 indicate that many molecular markers may be semivolatile, in this section, we investigate the effects of coupled gas-particle partitioning and chemical oxidation on molecular marker lifetime. Gas-phase oxidation can alter the gas-particle equilibrium, causing semivolatile material to evaporate.

Time-dependent evaporation and oxidation kinetics of species i can be written as:

$$\frac{dC_{p,i}}{dt} = -2\pi d_p DF(X_{m,i} KeC_i^o - C_{g,i})N_t - k_p C_{p,i}[\mathrm{OH}] \quad (6a)$$

$$\frac{dC_{g,i}}{dt} = 2\pi d_p DF(X_{m,i} KeC_i^o - C_{g,i})N_t - k_g C_{g,i}[\mathrm{OH}] \quad (6b)$$

Equation 6a and 6b track the concentration of compound i in the particle phase ($C_{p,i}$) and in the gas phase ($C_{g,i}$), respectively. The first term on the right-hand side in each equation describes mass transfer due to nonequilibrium gas-particle partitioning (net condensation or evaporation) and the second term on the right-hand side describes phase-specific chemistry. $X_{m,i}$ is the mass fraction of species i in the particle phase (= $C_{p,i}/C_{OA}$); hence, it also is time dependent. *Ke* is the Kelvin term that accounts for the increase in vapor pressure over a curved surface and is a function of the surface tension of bulk OA, calculated assuming a surface tension of σ = 0.05 N m^{-1}.[24] OH radical concentration [OH] is assumed to be 1 × 10^6 molecules cm^{-3}, a typical average value in the troposphere.[45] Rate constants for heterogeneous and homogeneous reactions are k_p and k_g, respectively. To predict the decay of $C_{p,i}$ and $C_{g,i}$, these equations were solved simultaneously for typical atmospheric conditions using a first-order backward-difference scheme and the set of inputs summarized in Table S1.

The heterogeneous oxidation rate constant k_p is related to the diffusion-corrected collision frequency between the oxidizing agent (here, assumed to be the OH radical) and the particles (see Supporting Information):

$$k_p = \frac{\gamma_{OH} J_{OH} MW_{OA}}{C_{OA} N_A} \quad (7)$$

where γ_{OH} is the OH radical uptake coefficient (assumed to be unity, the maximum theoretical value for this coefficient),[46,47] J_{OH} is the collision rate between the OH radical and the particles, MW_{OA} is the average molecular weight of the bulk OA (assumed to be 0.250 kg mol^{-1}), and N_A is Avogadro's number. For typical atmospheric conditions (C_{OA} = 5 μg m^{-3} and d_p = 200 nm at 25 °C), k_p is 7.5 × 10^{-13} cm^3 molecules^{-1} s^{-1} and is independent of specific chemical species, assuming the organic phase is well-mixed. The gas-phase reaction rate constant k_g is assumed to be 2 × 10^{-11} cm^3 molecules^{-1} s^{-1}, based on data for large saturated hydrocarbons.[48]

Figure 4 presents model predictions of the particle-phase decay of a set of hypothetical compounds spanning a broad range of volatilities from essentially nonvolatile (C_i^o (298 K) = 0.05 μg m^{-3}) to semivolatile (C_i^o (298 K) = 50 μg m^{-3}). The calculations were performed at a typical atmospheric organic aerosol concentration (C_{OA} = 5 μg m^{-3}) assuming the system forms an ideal solution (ζ_i = 1); therefore, each compound has a different fraction of material present in the gas phase (ranging from 0% for a truly nonvolatile species to 99%). The predicted decay rate of particle-phase material increases drastically with increasing gas-phase fraction because gas-phase oxidation is ~30 times faster than heterogeneous reactions. Gas-phase chemistry removes material via oxidation, causing particle-phase material to evaporate to maintain phase equilibrium, leading to additional gas-phase oxidation.

Figure 4 indicates that even a small fraction of material in the gas phase will dramatically increase the decay rate of the compound compared to a nonvolatile species. For example, 5α-cholestane (C_i^o (298 K) = 0.38 μg m^{-3}) will have a gas-phase fraction of ~10% for a typical urban atmosphere (defined above), resulting in a decay rate nearly 3 times faster than a nonvolatile compound (i.e., heterogeneous chemistry alone). The decay of levoglucosan (C_i^o (298 K) = 13 μg m^{-3}) would be even more rapid, due to the availability of more gas-phase material to be lost in oxidation reactions. Figure 4 indicates that the e-fold atmospheric lifetime of levoglucosan and 5α-cholestane, assuming equilibrium gas-particle partitioning and negligible deposition, are 0.21 and 2.0 days, respectively. In comparison, the e-fold atmospheric lifetime for a non-volatile species is > 5.5 days.

Figure 4 also compares the model predictions to experimental data of Hennigan et al.[16] for levoglucosan decay

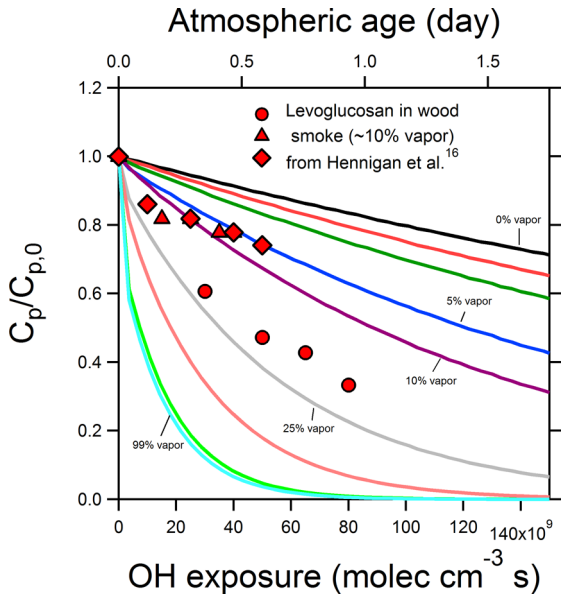

Figure 4. Effects of gas-particle partitioning on predicted particle-phase decay of individual organic compounds as a function of OH exposure, calculated using eq 6 using typical atmospheric conditions (see text). The *y*-axis represents the ratio of particle-phase concentration (C_p) to the initial particle-phase concentration ($C_{p,0}$). Each curve represents different gas-particle partitioning. Model predictions are compared to measured decay of levoglucosan from three different experiments indicated by symbols from Hennigan et al.[16] Atmospheric age is defined assuming a constant [OH] = 1 × 106 molecules cm^{-3}.

measured during the photo-oxidation of wood smoke aerosol. The measured decay is too fast to be explained by heterogeneous OH uptake to the particles; thus, Hennigan et al.[16] hypothesize that this was due to levoglucosan being semivolatile. Using the measured C_i^o for levoglucosan (Table 1) and the measured C_{OA} from Hennigan et al.,[16] we estimate that 10% of the levoglucosan was in the gas phase during those experiments. Figure 4 indicates that the measured decay of levoglucosan can be explained using eq 6 accounting for coupled oxidation and gas-particle partitioning. Weitkamp et al.[19] and Lambe et al.[17] also measured unexpectedly rapid decay of norhopane (C_{29} hopane) and 5α-cholestane, both of which are less volatile than levoglucosan. To explain the data of Weitkamp et al.[19] and Lambe et al.,[17] ζ_i would need to be greater than unity, consistent with the findings of Ruehl et al.[4]

Gas-Particle Partitioning in Ambient Aerosol. Even if C_i^o is known, gas-particle partitioning of individual organic compounds in ambient aerosols is challenging to model because the system may form a nonideal solution ($\zeta_i \neq 1$), or there may be multiple organic phases. ζ_i is a major uncertainty when extrapolating single-component data to the atmosphere, since it is dependent on bulk particle-phase composition. In the atmosphere, molecular marker compounds exist as part of a very complex (>10^4 individual organic compounds) organic matrix.[49] Building a model to predict the gas-particle partitioning in atmospheric aerosols is beyond the scope of this work; however, we can apply our experimentally derived saturation concentrations to build an understanding of partitioning behavior using simple systems. Nonpolar compounds (e.g., hopanes, steranes, and many other molecular markers) are expected to have $\zeta_i > 1$ for atmospheric systems dominated by secondary organic aerosol.[4,32] If $\zeta_i > 1$, then the C_i^o values in Table 1 under-estimate the equilibrium vapor phase concentrations. To illustrate the potential effects of nonideality, we assume that there is a single OA phase containing 48 wt % reduced hydrocarbons (e.g., primary organic aerosol), 48 wt % oxygenated organics (e.g., secondary organic aerosol), and 4 wt % 5α-cholestane. We can predict the activity coefficient for 5α-cholestane using the Aerosol Inorganic−Organic Mixtures Functional groups Activity Coefficients Model (AIOMFAC).[50−52] Using *n*-tetracosane (C_{24} *n*-alkane) as a surrogate for the reduced hydrocarbon phase and adipic acid (C_6 diacid) for the oxygenated organics, the model predicts $\zeta_{5\alpha\text{-cholestane}} \approx 9.2$; hence, the effective saturation concentration (C_i^*) for 5α-cholestane in this system is ~3.5 μg m^{-3} (eq 3), which is consistent with the estimates of Ruehl et al.[4] Furthermore, if we assume that ambient C_{OA} contains two phases (e.g., liquid-like reduced primary organic aerosol and semisolid oxygenated secondary organic aerosol), C_{OA} is effectively reduced since 5α-cholestane will likely only partition into the reduced phase. Consequently, more 5α-cholestane will be present in the gas phase, following eq 4. This analysis suggests that future source apportionment studies may require the mixing state of ambient OA to provide the fraction of the bulk OA into which a given organic molecular marker will partition as well as an estimate of the activity coefficient to assess nonidealities in the solution.

Temperature also impacts the phase partitioning of molecular markers. For example, levoglucosan present in residential wood burning emissions at colder wintertime temperatures will favor the particle phase (>90% in particle phase; C_i^o (T = 273 K) = 0.35 μg m^{-3}), while levoglucosan emitted by summertime wildfires will more likely to exist in the gas phase (~5% in particle phase; C_i^o (T = 313 K) = 85 μg m^{-3}). Hence, temperature-driven changes in phase partitioning will make molecular markers more susceptible during the summertime, potentially creating seasonal biases in source apportionment estimates.[2,53]

Presence of an *ad*sorbing phase (e.g., soot in diesel emissions) will also affect gas-particle partitioning. Studies have shown that soot will effectively reduce the saturation concentration of PAHs in ambient aerosol.[54,55] Furthermore, Ruehl et al.[4] propose that a nonabsorbing phase may account for reduced evaporation of certain organic compounds in rural and winter experiments. This may influence the lifetime of some molecular markers.

DISCUSSION

Our results show that several of the widely used organic molecular markers, such as levoglucosan and 5α-cholestane, may be semivolatile under atmospheric conditions (with C_{OA} = 5 μg m^{-3} and T = 298 K), assuming an ideal, well-mixed, liquid-like bulk OA; however, phase partitioning is sensitive to changes in both C_{OA} and T. While we have not directly investigated all organic molecular markers, we hypothesize that many other compounds are semivolatile under these conditions as well. In addition, multiple OA phases forming nonideal solutions may cause the molecular markers to be even more volatile.

Figure 4 demonstrates that a simple model that accounts for both partitioning and gas-phase oxidation explains some of the rapid particle-phase depletion observed in laboratory oxidation studies[16,17,19] and ambient data.[2] Kinetic calculations presented in Figure 4 indicate that semivolatile compounds undergo accelerated chemical oxidation (compared to nonvolatile

compounds) even if only 5% of the material is present in the gas phase. Therefore, concentrations of semivolatile molecular markers will rapidly decay in the atmosphere. This may potentially lead to a significant negative bias in source apportionment models using all but the least volatile organic markers.

For an atmosphere with a single, well-mixed, absorbing phase with C_{OA} = 5 μg m^{-3}, Figure 4 indicates that compounds must have C_i^o (298 K) < 0.05 μg m^{-3} (<1% in gas phase, effectively nonvolatile) to not experience accelerated oxidation rates. The only compounds investigated in this work that may be classified as "nonvolatile" are cholesterol and *n*-triacontane. However, even these species will be heterogeneously oxidized in the atmosphere.[18,19] If these species do not form an ideal solution with the organic aerosol matrix ($\zeta_i \neq 1$), then they may also be susceptible to more rapid oxidation.

During source sampling, molecular markers may appear to be nonvolatile since POA concentrations (even with dilution samplers) are often very high (hundreds of μg m^{-3}), which favors the particle phase.[56] Furthermore, quartz filters collect both particle- and gas-phase material. However, particle-phase concentrations will change as POA emissions leave the tailpipe and are rapidly diluted with background air, shifting gas-particle partitioning of semivolatile species to the gas-phase. Therefore, new approaches may be necessary to accurately account for the atmospheric evolution of molecular markers in source apportionment models.

■ ASSOCIATED CONTENT

Supporting Information

The Supporting Information contains figures of the graphical validation of the equilibrium condition in the TD, additional experimental data for organic molecular markers, and derivation of the heterogeneous reaction rate constant. This material is available free of charge via the Internet at http://pubs.acs.org.

■ AUTHOR INFORMATION

Corresponding Author

*E-mail: alr@andrew.cmu.edu.

Notes

The authors declare no competing financial interest.

■ ACKNOWLEDGMENTS

This research was supported by the National Science Foundation under grant ATM-0748402 and by the STAR Research Assistance Agreement RD834554 awarded by the U.S. Environmental Protection Agency. It has not been formally reviewed by the EPA. The views expressed in this document are solely those of the recipient, and the EPA does not endorse any products or commercial services mentioned in this publication. We also thank our anonymous reviewers for their constructive comments.

■ REFERENCES

(1) Schauer, J. J.; Rogge, W. F.; Hildemann, L. M.; Mazurek, M. A.; Cass, G. R.; Simoneit, B. R. T. Source apportionment of airborne particulate matter using organic compounds as tracers. *Atmos. Environ.* **1996**, *30* (22), 3837−3855.

(2) Robinson, A. L.; Donahue, N. M.; Rogge, W. F. Photochemical oxidation and changes in molecular composition of organic aerosol in the regional context. *J. Geophys. Res.-Atmos.* **2006**, *111*, (*D3*).

(3) Sihabut, T.; Ray, J.; Northcross, A.; McDow, S. R. Sampling artifact estimates for alkanes, hopanes, and aliphatic carboxylic acids. *Atmos. Environ.* **2005**, *39* (37), 6945−6956.

(4) Ruehl, C. R.; Ham, W. A.; Kleeman, M. J. Temperature-induced volatility of molecular markers in ambient airborne particulate matter. *Atmos. Chem. Phys.* **2011**, *11* (1), 67−76.

(5) Booth, A. M.; Montague, W. J.; Barley, M. H.; Topping, D. O.; McFiggans, G.; Garforth, A.; Percival, C. J. Solid state and sub-cooled liquid vapour pressures of cyclic aliphatic dicarboxylic acids. *Atmos. Chem. Phys.* **2011**, *11* (2), 655−665.

(6) Cappa, C. D.; Lovejoy, E. R.; Ravishankara, A. R. Evaporation rates and vapor pressures of the even-nunibered C(8)-C(18) monocarboxylic acids. *J. Phys. Chem. A* **2008**, *112* (17), 3959−3964.

(7) Chickos, J. S.; Webb, P.; Nichols, G.; Kiyobayashi, T.; Cheng, P. C.; Scott, L. The enthalpy of vaporization and sublimation of corannulene, coronene, and perylene at T=298.15 K. *J. Chem. Thermodyn.* **2002**, *34* (8), 1195−1206.

(8) Hanshaw, W.; Nutt, M.; Chickos, J. S. Hypothetical thermodynamic properties. Subcooled vaporization enthalpies and vapor pressures of polyaromatic hydrocarbons. *J. Chem. Eng. Data* **2008**, *53* (8), 1903−1913.

(9) Lei, Y. D.; Chankalal, R.; Chan, A.; Wania, F. Supercooled liquid vapor pressures of the polycyclic aromatic hydrocarbons. *J. Chem. Eng. Data* **2002**, *47* (4), 801−806.

(10) Mokbel, I.; Ruzicka, K.; Majer, V.; Ruzicka, V.; Ribeiro, M.; Jose, J.; Zabransky, M. Vapor pressures and thermal data for three high-boiling compounds of petroleum interest: 1-phenyldodecane, (5 alpha)-cholestane, adamantane. *Fluid Phase Equilib.* **2000**, *169* (2), 191−207.

(11) Nichols, G.; Kweskin, S.; Frericks, M.; Reiter, S.; Wang, G.; Orf, J.; Carvallo, B.; Hillesheim, D.; Chickos, J. Evaluation of the vaporization, fusion, and sublimation enthalpies of the 1-alkanols: The vaporization enthalpy of 1-, 6-, 7-, and 9-heptadecanol, 1-octadecanol, 1-eicosanol, 1-docosanol, 1-hexacosanol, and cholesterol at T 298.15 K by correlation gas chromatography. *J. Chem. Eng. Data* **2006**, *51* (2), 475−482.

(12) Oja, V.; Chen, X.; Hajaligol, M. R.; Chan, W. G. Sublimation Thermodynamic Parameters for Cholesterol, Ergosterol, beta-Sitosterol, and Stigmasterol. *J. Chem. Eng. Data* **2009**, *54* (3), 730−734.

(13) Oja, V.; Suuberg, E. M. Vapor pressures and enthalpies of sublimation of D-glucose, D-xylose, cellobiose, and levoglucosan. *J. Chem. Eng. Data* **1999**, *44* (1), 26−29.

(14) Tang, I. N.; Munkelwitz, H. R. Determination of Vapor-Pressure from Droplet Evaporation Kinetics. *J. Colloid Interface Sci.* **1991**, *141* (1), 109−118.

(15) Rudich, Y.; Donahue, N. M.; Mentel, T. F. Aging of organic aerosol: Bridging the gap between laboratory and field studies. *Annu. Rev. Phys. Chem.* **2007**, *58*, 321−352.

(16) Hennigan, C. J.; Sullivan, A. P.; Collett, J. L.; Robinson, A. L. Levoglucosan stability in biomass burning particles exposed to hydroxyl radicals. *Geophys. Res. Lett.* **2010**, *37*.

(17) Lambe, A. T.; Miracolo, M. A.; Hennigan, C. J.; Robinson, A. L.; Donahue, N. M. Effective Rate Constants and Uptake Coefficients for the Reactions of Organic Molecular Markers (n-Alkanes, Hopanes, and Steranes) in Motor Oil and Diesel Primary Organic Aerosols with Hydroxyl Radicals. *Environ. Sci. Technol.* **2009**, *43* (23), 8794−8800.

(18) Weitkamp, E. A.; Hartz, K. E. H.; Sage, A. M.; Donahue, N. M.; Robinson, A. L. Laboratory measurements of the heterogeneous oxidation of condensed-phase organic molecular makers for meat cooking emissions. *Environ. Sci. Technol.* **2008**, *42* (14), 5177−5182.

(19) Weitkamp, E. A.; Lambe, A. T.; Donahue, N. M.; Robinson, A. L. Laboratory Measurements of the Heterogeneous Oxidation of Condensed-Phase Organic Molecular Makers for Motor Vehicle Exhaust. *Environ. Sci. Technol.* **2008**, *42* (21), 7950−7956.

(20) Saleh, R.; Walker, J.; Khlystov, A. Determination of saturation pressure and enthalpy of vaporization of semi-volatile aerosols: The integrated volume method. *J. Aerosol Sci.* **2008**, *39* (10), 876−887.

(21) Veranth, J. M.; Gelein, R.; Oberdorster, G. Vaporization-condensation generation of ultrafine hydrocarbon particulate matter

for inhalation toxicology studies. *Aerosol Sci. Technol.* **2003**, *37* (7), 603−609.
(22) Saleh, R.; Khlystov, A.; Shihadeh, A. Effect of Aerosol Generation Method on Measured Saturation Pressure and Enthalpy of Vaporization for Dicarboxylic Acid Aerosols. *Aerosol Sci. Technol.* **2010**, *44* (4), 302−307.
(23) Yaws, C. L. *Yaws' Critical Property Data for Chemical Engineers and Chemists*; Knovel, 2012.
(24) Riipinen, I.; Pierce, J. R.; Donahue, N. M.; Pandis, S. N. Equilibration time scales of organic aerosol inside thermodenuders: Evaporation kinetics versus thermodynamics. *Atmos. Environ.* **2010**, *44* (5), 597−607.
(25) Saleh, R.; Shihadeh, A.; Khlystov, A. On transport phenomena and equilibration time scales in thermodenuders. *Atmos. Meas. Tech.* **2011**, *4* (3), 571−581.
(26) Chickos, J. S.; Hanshaw, W. Vapor pressures and vaporization enthalpies of the n-alkanes from C-31 to C-38 at T=298.15 K by correlation gas chromatography. *J. Chem. Eng. Data* **2004**, *49* (3), 620−630.
(27) Chickos, J. S.; Hanshaw, W. Vapor pressures and vaporization enthalpies of the n-alkanes from C-21 to C-30 at T=298.15 K by correlation gas chromatography. *J. Chem. Eng. Data* **2004**, *49* (1), 77−85.
(28) Morgan, D. L.; Kobayashi, R. Direct Vapor-Pressure Measurements of 10 N-Alkanes in the C-10-C(28) Range. *Fluid Phase Equilib.* **1994**, *97*, 211−242.
(29) McCabe, C.; Jackson, G. SAFT-VR modelling of the phase equilibrium of long-chain n-alkanes. *Phys. Chem. Chem. Phys.* **1999**, *1* (9), 2057−2064.
(30) Sasse, K.; Jose, J.; Merlin, J. C. A Static Apparatus for Measurement of Low Vapor-Pressures - Experimental Results on High Molecular-Weight Hydrocarbons. *Fluid Phase Equilib.* **1988**, *42*, 287−304.
(31) Piacente, V.; Fontana, D.; Scardala, P. Enthalpies of Vaporization of a Homologous Series of N-Alkanes Determined from Vapor-Pressure Measurements. *J. Chem. Eng. Data* **1994**, *39* (2), 231−237.
(32) Donahue, N. M.; Epstein, S. A.; Pandis, S. N.; Robinson, A. L. A two-dimensional volatility basis set: 1. organic-aerosol mixing thermodynamics. *Atmos. Chem. Phys.* **2011**, *11* (7), 3303−3318.
(33) Donahue, N. M.; Robinson, A. L.; Stanier, C. O.; Pandis, S. N. Coupled partitioning, dilution, and chemical aging of semivolatile organics. *Environ. Sci. Technol.* **2006**, *40* (8), 2635−2643.
(34) Safieddine, S. *Experimental Validation of an Integrated Volume-Tandem Differential Mobility Analysis Method for Determining Thermodynamic and Kinetic Properties of Semi-Volatile Organic Aerosols*; American University of Beiruit, 2011.
(35) Rader, D. J.; McMurry, P. H.; Smith, S. Evaporation Rates of Monodisperse Organic Aerosols in the 0.02-Mu-M-Diameter to 0.2-Mu-M-Diameter Range. *Aerosol Sci. Technol.* **1987**, *6* (3), 247−260.
(36) Oja, V.; Suuberg, E. M. Vapor pressures and enthalpies of sublimation of polycyclic aromatic hydrocarbons and their derivatives. *J. Chem. Eng. Data* **1998**, *43* (3), 486−492.
(37) Wakayama, N.; Inokuchi, H. Heats of Sublimation of Polycyclic Aromatic Hydrocarbons and Their Molecular Packings. *Bull. Chem. Soc. Jpn.* **1967**, *40* (10), 2267.
(38) Grieshop, A. P.; Donahue, N. M.; Robinson, A. L. Laboratory investigation of photochemical oxidation of organic aerosol from wood fires 2: Analysis of aerosol mass spectrometer data. *Atmos. Chem. Phys.* **2009**, *9* (6), 2227−2240.
(39) Huffman, J. A.; Docherty, K. S.; Mohr, C.; Cubison, M. J.; Ulbrich, I. M.; Ziemann, P. J.; Onasch, T. B.; Jimenez, J. L. Chemically-Resolved Volatility Measurements of Organic Aerosol from Different Sources. *Environ. Sci. Technol.* **2009**, *43* (14), 5351−5357.
(40) Hennigan, C. J.; Miracolo, M. A.; Engelhart, G. J.; May, A. A.; Presto, A. A.; Lee, T.; Sullivan, A. P.; McMeeking, G. R.; Coe, H.; Wold, C. E.; Hao, W. M.; Gilman, J. B.; Kuster, W. C.; de Gouw, J.; Schichtel, B. A.; Collett, J. L.; Kreidenweis, S. M.; Robinson, A. L. Chemical and physical transformations of organic aerosol from the photo-oxidation of open biomass burning emissions in an environmental chamber. *Atmos. Chem. Phys.* **2011**, *11* (15), 7669−7686.
(41) Lee, T.; Sullivan, A. P.; Mack, L.; Jimenez, J. L.; Kreidenweis, S. M.; Onasch, T. B.; Worsnop, D. R.; Malm, W.; Wold, C. E.; Hao, W. M.; Collett, J. L. Chemical Smoke Marker Emissions During Flaming and Smoldering Phases of Laboratory Open Burning of Wildland Fuels. *Aerosol Sci. Technol.* **2010**, *44* (9), I−V.
(42) Grieshop, A. P.; Miracolo, M. A.; Donahue, N. M.; Robinson, A. L. Constraining the Volatility Distribution and Gas-Particle Partitioning of Combustion Aerosols Using Isothermal Dilution and Thermodenuder Measurements. *Environ. Sci. Technol.* **2009**, *43* (13), 4750−4756.
(43) Ziemann, P. J.; Faulhaber, A.; Huffman, J. A.; Lechner, M. J.; Jimenez, J. L. *Combined Mass Spectra-Volatility Database*. http://cires.colorado.edu/jimenez-group/TDPBMSsd/.
(44) Cubison, M. J.; Ortega, A. M.; Hayes, P. L.; Farmer, D. K.; Day, D.; Lechner, M. J.; Brune, W. H.; Apel, E.; Diskin, G. S.; Fisher, J. A.; Fuelberg, H. E.; Hecobian, A.; Knapp, D. J.; Mikoviny, T.; Riemer, D.; Sachse, G. W.; Sessions, W.; Weber, R. J.; Weinheimer, A. J.; Wisthaler, A.; Jimenez, J. L. Effects of aging on organic aerosol from open biomass burning smoke in aircraft and laboratory studies. *Atmos. Chem. Phys.* **2011**, *11* (23), 12049−12064.
(45) Seinfeld, J. H.; Pandis, S. N. *Atmospheric Chemistry and Physics from Air Pollution to Climate Change* , 2nd ed.; J. Wiley: Hoboken, NJ, 2006; pp xxviii, 1203 pp.
(46) Bertram, A. K.; Ivanov, A. V.; Hunter, M.; Molina, L. T.; Molina, M. J. The reaction probability of OH on organic surfaces of tropospheric interest. *J. Phys. Chem. A* **2001**, *105* (41), 9415−9421.
(47) Worsnop, D. R.; Morris, J. W.; Shi, Q.; Davidovits, P.; Kolb, C. E. A chemical kinetic model for reactive transformations of aerosol particles. *Geophys. Res. Lett.* **2002**, *29*, 20.
(48) Kwok, E. S. C.; Atkinson, R. Estimation of Hydroxyl Radical Reaction-Rate Constants for Gas-Phase Organic-Compounds Using a Structure-Reactivity Relationship - an Update. *Atmos. Environ.* **1995**, *29* (14), 1685−1695.
(49) Goldstein, A. H.; Galbally, I. E. Known and unexplored organic constituents in the earth's atmosphere. *Environ. Sci. Technol.* **2007**, *41* (5), 1514−1521.
(50) Zuend, A.; Marcolli, C.; Booth, A. M.; Lienhard, D. M.; Soonsin, V.; Krieger, U. K.; Topping, D. O.; McFiggans, G.; Peter, T.; Seinfeld, J. H. New and extended parameterization of the thermodynamic model AIOMFAC: Calculation of activity coefficients for organic-inorganic mixtures containing carboxyl, hydroxyl, carbonyl, ether, ester, alkenyl, alkyl, and aromatic functional groups. *Atmos. Chem. Phys.* **2011**, *11* (17), 9155−9206.
(51) Zuend, A.; Marcolli, C.; Luo, B. P.; Peter, T. A thermodynamic model of mixed organic-inorganic aerosols to predict activity coefficients. *Atmos. Chem. Phys.* **2008**, *8* (16), 4559−4593.
(52) Aerosol Inorganic-Organic Mixtures Functional groups Activity Coefficients Model. http://www.aiomfac.caltech.edu.
(53) Subramanian, R.; Donahue, N. M.; Bernardo-Bricker, A.; Rogge, W. F.; Robinson, A. L. Insights into the primary-secondary and regional-local contributions to organic aerosol and PM2.5 mass in Pittsburgh, Pennsylvania. *Atmos. Environ.* **2007**, *41* (35), 7414−7433.
(54) Accardi-Dey, A.; Gschwend, P. M. Reinterpreting literature sorption data considering both absorption into organic carbon and adsorption onto black carbon. *Environ. Sci. Technol.* **2003**, *37* (1), 99−106.
(55) Dachs, J.; Eisenreich, S. J. Adsorption onto aerosol soot carbon dominates gas-particle partitioning of polycyclic aromatic hydrocarbons. *Environ. Sci. Technol.* **2000**, *34* (17), 3690−3697.
(56) Robinson, A. L.; Grieshop, A. P.; Donahue, N. M.; Hunt, S. W. Updating the Conceptual Model for Fine Particle Mass Emissions from Combustion Systems. *J. Air Waste Manage.* **2010**, *60* (10), 1204−1222.
(57) Simoneit, B. R. T.; Schauer, J. J.; Nolte, C. G.; Oros, D. R.; Elias, V. O.; Fraser, M. P.; Rogge, W. F.; Cass, G. R. Levoglucosan, a tracer for cellulose in biomass burning and atmospheric particles. *Atmos. Environ.* **1999**, *33* (2), 173−182.

(58) Rogge, W. F.; Hildemann, L. M.; Mazurek, M. A.; Cass, G. R.; Simoneit, B. R. T. Sources of fine organic aerosol. 1. Charbroilers and meat cooking operations. *Environ. Sci. Technol.* **1991**, *25* (6), 1112−1125.
(59) Rogge, W. F.; Hildemann, L. M.; Mazurek, M. A.; Cass, G. R.; Simoneit, B. R. T. Sources of fine organic aerosol. 2. Noncatalyst and catalyst-equipped automobiles and heavy-duty diesel trucks. *Environ. Sci. Technol.* **1993**, *27* (4), 636−651.